Analytical Methods

CRITICAL REVIEW

View Article Online
View Journal

CrossMark click for updates

Cite this: DOI: 10.1039/c6ay00293e

Analytical methodologies using carbon substrates developed by pyrolysis

Tomás E. Benavidez,[a] Rodrigo Martinez-Duarte[b] and Carlos D. Garcia*[a]

As a viable alternative with respect to carbon-based materials prepared by vapor deposition, the pyrolysis of non-volatile organic precursors has allowed the development of substrates with advantageous properties towards the development of sensors. Considering the importance and versatility of these materials, this review provides a summary of representative articles describing the procedures and most important considerations linked to the fabrication of these films, and their characterization in terms of structure, thickness, topography, contact angle, as well as optical and electrochemical properties. The review focuses on analytical applications such as electroanalysis, biosensors, dielectrophoresis, and solid phases for separations published in the last five years but additional contributions outside this period have been included to provide readers background information to link the chemical functionality of the films with the corresponding performance. A series of promising directions for the future of the field are also described.

Received 29th January 2016
Accepted 1st April 2016

DOI: 10.1039/c6ay00293e

www.rsc.org/methods

Published on 01 April 2016. Downloaded by Clemson University on 15/04/2016 14:03:16.

1. Introduction

Without a question, the number of reports describing analytical applications of carbon paste,[1,2] glassy carbon,[3,4] boron-doped diamond,[5,6] highly oriented pyrolytic graphite,[7] carbon fibers, carbon ink,[8] carbon black, carbon nanotubes,[9,10] fullerenes, nanohorns, graphene,[11,12] and carbon dots[13,14] has increased tremendously over the last two decades. Carbon is no longer limited to electrochemical detectors and has been extensively applied, for example, to improve sample preconcentration and separation techniques.[15–17] In fact, a quick literature survey shows an average of more than 100 000 papers related to analytical applications of carbon are published almost every year. Although this could suggest the approach of an stagnation stage in the field, it is clear that a variety of modern methods and techniques now enable challenging long-established models and identifying key features for further exploration.[18] Moreover, the unique properties of carbon[19] and the versatility of current fabrication methods continue opening new doors for the development of innovative applications that clearly transcend the boundaries of research laboratories (*e.g.* molecular electronics[20]). In terms of analytical applications, carbon offers a variety of advantages with respect to other materials including

[a]*Department of Chemistry, Clemson University, 219 Hunter Laboratories, Clemson, SC 29634, USA. E-mail: cdgarci@clemson.edu; Fax: +1-864-656-6613; Tel: +1-864-656-1356; +1-864-656-3065*

[b]*Department of Mechanical Engineering, Clemson University, Clemson, SC 29634, USA*

Tomas E. Benavidez graduated with a BS in Biochemistry (2004) and a PhD in Chemistry (2010) from the National University of Cordoba, Argentina under the supervision of Dr. Baruzzi. Dr. Benavidez performed post-doctoral studies with Dr. Schmickler and Dr. Santos at Universität Ulm (Germany). He is now interested in understanding the role of adsorbed macromolecules to nanomaterials.

Rodrigo Martinez-Duarte graduated from the Tecnologico de Monterrey, Mexico (BS, 2004) and continued his studies at University of California, Irvine (MS, 2009 – PhD, 2010). He then performed postdoctoral studies at Ecole Polytechnique Federale de Lausanne (EPFL) in Lausanne, Switzerland. He joined Clemson University in 2013 as an Assistant Professor. His expertise lies at the interface between micro/nanofabrication, carbonaceous materials, electrokinetics and microfluidics.

Published on 01 April 2016. Downloaded by Clemson University on 15/04/2016 14:03:16.

relatively clean electrochemistry (good electrocatalytic activity and low background currents), large surface area, a rich and versatile surface chemistry, and good electrical conductivity. While a large proportion of literature relates to the use and modification of traditional carbon electrodes (glassy carbon or paste) or the use of carbon-based materials attached to the surface of metallic electrodes, the development of thin carbon films by pyrolytic reactions of a deposited organic layer has gained significant attention in the last few years. Therefore, and considering the importance of these electrodes, the present review provides a summary of representative articles describing the use of carbon substrates prepared by pyrolysis of a solid organic material, linking the properties of the material with the analytical methodologies developed thereof. The review focuses on applications published in the last five years but additional contributions outside this period have been included to provide readers background information to link the chemical functionality of the films with the corresponding analytical applications.

2. Fabrication and characterization of carbon films

2.1 Formation mechanism

Considering that carbon has the highest sublimation point of all elements (3825 °C),† two main routes have been utilized to produce carbon substrates by pyrolysis. The first alternative (bottom-up) is to produce films by the generation of elementary carbon (by thermal decomposition of gaseous hydrocarbons or arc-discharge at graphitic electrodes) and recombination to form solid carbon structures. This process is known as chemical vapor deposition (CVD) and yields to the formation of what most papers refer to as pyrolytic carbon, amorphous carbon, or diamond-like carbon.[21] The mechanism involved in the formation of pyrolytic carbon substrates has been extensively investigated and may involve more than 250 species[22] taking part in a myriad of almost 1200 reversible reactions.[23] In a nutshell, CVD involves the use of high temperature and an organic gaseous feedstock (such as methane and acetylene) that dissociate and form molecular species (ethane, ethene, ethine, propine, allene, vinylethine) as well as a number of radicals.[24] As a reference point for the selection of the temperature, it is worth mentioning that the thermal dissociation of CH_4 occurs in the 500–1000 °C range.[24] For this reason, and although the selection of the temperature required to produce pyrolytic carbon films by CVD can be influenced by a number of variables,[25] the furnace is typically set within the 800–1100 °C range.[26,27] Upon recombination, the compounds originate the so-called *first aromatic ring* (benzene and substituted benzenes), *via* a low temperature C_4-route, with butadienyl as the intermediate. This process is followed by *aromatic growth*, a process in which a series of five- and six-member rings are condensed and converted (through isomerization, hydrogen migration, and reaction with low-MW species such as ethine) into clusters of polyaromatic hydrocarbons (PAH). These processes are described by the HACA-mechanism (hydrogen abstraction and carbon addition) and aromatic condensation (aryl–aryl combination followed by dehydrocyclization). As an early example of an analytical application of this type of films, it is worth mentioning a report from Blaedel and Mabbott,[28] who placed a pre-heated quartz rod into a stream of natural gas and produced black shiny surfaces that were used for the electrochemical oxidation of NADH. It is also important to point out that a key aspect involving the development of pyrolytic carbon substrates by CVD, especially if materials with larger ratios of sp^2-hybridized carbon are sought, is the requirement of metallic nanoparticles (usually Cu, Ni, Fe, Co, and/or Mo) to act as catalyst. Although these particles can act as nucleation points for low-MW carbon molecules to assemble and grow into graphitic structures,[29] the overall efficiency of the method is rather low (around 20% conversion yielding a mixture of structures).[30] Reviews describing similar mechanisms leading to the formation of fullerenes[31] and other carbon nanoallotropes[32] as well as analytical applications have been presented.[10,15,33] Also taking advantage of the decomposition of low-MW precursors, spray pyrolysis has been extensively used for the development of powdered carbon nanomaterials.[34]

With slight differences with respect to the mechanism involved in CVD, the second alternative to produce carbon substrates, and the focus of attention in this review, is the uncatalyzed pyrolytic treatment of substrates pre-coated with a layer of an organic precursor (top-down). This approach yields to glass-like carbon[21] (also known as the trademarks "glassy carbon" and "vitreous carbon") and provides researchers a much richer selection of starting materials to tune the properties of the resulting substrates and a source-to-product efficiency that can reach 70%.[35] In general, the fabrication processes involves a high-temperature pyrolysis step (under a controlled atmosphere) of some solid, non-volatile, organic material. Although the first pertinent report of a synthetic carbon material was produced by pyrolysis of a phenolic resin,[36] the overall strategy gained importance after a paper from

† http://www.rsc.org/periodic-table/element/6/carbon.

Carlos D. Garcia received his B.S. in Biochemistry (1996) and Ph.D. in Chemistry (2001) from the National University of Cordoba, Argentina. He then performed postdoctoral studies at Mississippi State University and Colorado State University and started his independent career at UT San Antonio. In August 2015 he joined Clemson University as Professor of Chemistry. With the goal of improving the performance of sensing devices, his research program is focused on the development and characterization of microfluidics as well as understanding the interactions between nanostructured materials and biomolecules.

This journal is © The Royal Society of Chemistry 2016

Published on 01 April 2016. Downloaded by Clemson University on 15/04/2016 14:03:16.

Davidson,[37] who demonstrated the possibility of preparing carbon films from cellulose. Only seven years later, it was noted that materials prepared by pyrolysis of other substrates (such as phenolic resins, polyfurfuryl alcohol, or polyvynilidene chloride) displayed very similar properties.[38] The structure of glassy carbon can be described as a number of layers of tangled ribbons,[39,40] similar to those found in graphite but without the corresponding extensive, oriented sheets of sp^2 carbon. This model is compatible with most of the properties of the resulting materials and has been described using a number of computational tools, including Monte Carlo simulations.[41] The overall mechanism for the pyrolysis reaction has been extensively described for cellulose and progresses in several distinctive stages that sequentially occur as the temperature increases. First, a slight weigh loss is typically observed when the temperature reaches approximately 115 °C. This process is typically attributed to the release of water and other adsorbed species. Release of methane, carboxyl, carbonyls, and hydrogen (favoring the formation of volatile compounds[42]) occurs at temperatures in the range of 250–500 °C and yields to significant losses in weight, shrinking, and coalescence of polymeric chains. The kinetics of this step can be described by the Broido–Shafizadeh (B–S) mechanism.[43] Upon further elimination of hydrogen, at temperatures in the 600–700 °C range, the weight of the product (determining the overall yield of the process) is typically stabilized. As the result of the crosslinking of polymeric chains, formation of graphitic domains,[44] and a reduction in pore size,[45] more compact structures with increased conductivity are obtained in the 700–900 °C range.[46,47] These stages can be clearly identified by thermogravimetric analysis (TGA) and are significantly influenced by the chemical composition of the starting material.[35,48] It is also important to note that the C–C bonds in the polymer backbone do not break at these temperatures, so the carbon source can only form graphitic planes of limited dimensions, with L_a (size of the layer plane) and L_c (crystallite size) in the range of 30 to 70 Å.[49] Although not typically reported for analytical applications, further reductions in structural defects and more extensive graphitization have been reported by annealing the substrate above 1500 °C or 2500 °C, respectively.[50,51]

2.2 Considerations for the pyrolysis step

Because it is simpler to flush the system with a gas than maintaining vacuum (10^{-6} to 10^{-7} Torr),[52] the vast majority of the films are produced in an inert atmosphere. Working at low pressures also requires the use of thicker tubes in the furnace, which adds to the expense and limits the heating/cooling rates. Therefore, pyrolysis reactions are typically carried out in atmospheres of argon,[53] helium,[54] or nitrogen.[51] To avoid potential oxidation reactions and promote the formation of hydrogen-terminated clusters, a large percentage of authors have elected to use slightly reductive conditions (95% Ar–5% H_2).[35,55–57] Along with the H_2 released during the pyrolysis step, the hydrogen introduced in the forming gas may also play a role in both the growth of crystallites and the removal of oxygen from the matrix.[58] Gas mixtures containing higher amounts of hydrogen[59,60] have been reported but are unlikely justified due the increased flammability of the gas and the corresponding safety risks.[61] For the specific cases of pyrolytic carbon[62] and carbon nanotubes,[63] it has been also reported that the addition of H_2O to the reaction chamber can significantly increase the growth rate with respect to that obtained with traditional mixtures of precursors. To the best of our knowledge, this possibility has not been recently explored in the fabrication of glassy carbon. Unless specific conditions for the pyrolysis are required, gas mixtures can be obtained from commercial suppliers and connected to the furnace *via* a standard regulator. For experiments requiring precise control of the flow rate, or variable composition of the forming gas, one of the most convenient alternatives is to incorporate flow controllers in the design. Although these controllers are rather expensive (>$1500 each, at least two needed), a variety of sources are currently available (*e.g.* Sierra; Monterrey, CA, USA). Being compatible with H_2, 304 or 316 grade stainless steel tubing are probably the best choices for gas lines. Users should be aware that other materials (such as copper) can become brittle in the presence of hydrogen and pose a fire hazard.[64] Using *ad hoc* fittings (*e.g.* MTI; Richmond, CA, USA), the gas lines are typically connected to a tube made of either hard-fired alumina or fused quartz. While the former allows heating up to 1800 °C, these tubes are opaque and can be easily broken by thermal stress (heating/cooling rates should not exceed 5 °C min^{-1}). The latter tubes can only go to 1200 °C (but much lower temperatures are recommended if vacuum is applied) and allow visual inspection of the process. The technology behind the hardware used in tube furnaces is mature at this point and most laboratory supply companies offer models that can reach 1000–1200 °C using either fixed (around 10 °C min^{-1})[65,66] or programmable temperature ramps.[67,68] In this regard, R. Compton's group also reported that electrodes synthesized by a much faster thermal process (ramping at 140 °C min^{-1}) showed one of the lowest resistivities reported for this kind of material (AZ 4562, *ca.* 4–6 $\times$ 10^{-3} Ω cm) but were slightly rougher than electrodes fabricated using slower thermal ramps.[69] Besides the obvious safety precautions when dealing with H_2 and high-temperatures, users should consider that adequate power (>5000 W) and an exhaust line (to vent unreacted H_2 and volatile compounds) must be available. As the pyrolysis generates a number of compounds (furfurals, aldehydes, *etc.*) that tend to adhere to the cooler parts of the tube, frequent cleaning is recommended. Fortunately, this step can be accomplished by simply operating the furnace in the presence of air (opening the ends of the tube), carefully sliding the tube from one side to the other to minimize thermal stress.

2.3 Selection of material sources

Just like the choices for carbon feedstocks used in CVD are virtually infinite,[70] a wide variety of materials can be pyrolyzed to yield glassy-carbon substrates. Since the initial reports describing the possibility to form carbon films from phenolic resins[36] or cellulose,[37] a number of organic materials have been used towards the development of carbon-based substrates[71] and

Published on 01 April 2016. Downloaded by Clemson University on 15/04/2016 14:03:16.

many more are regularly published in the literature (*i.e.* banana stems, insects, grass, cookies, chocolate, and even animal feces[72,73]). Due to the possibility to form uniform films with controlled properties, photoresists are probably the most used sources to fabricate substrates for analytical applications. Under this category, SU-8 (commercially available from Microchem Corp; Westborough, MA, USA or Gersteltec; Pully, Switzerland) is one of the most commonly reported materials.[56,66,74] SU-8 is a negative photoresist composed of a bisphenol A – epichlorohydrin – formaldehyde copolymer[57] that can yield high aspect ratio structures and does not reflow under pyrolysis. This photoresist also has excellent adhesion properties to non-conductive substrates (like SiO_2) and has enabled the development of a number of patterned structures including interdigitated arrays[75,76] or a series of stacked carbon electrodes fabricated using multiple UV-lithography processes and a single pyrolysis step.[77] Using SU-8 as a benchmark, Madou's group examined the electrical property changes and shrinkage of AZ P4620 (AZ Electronic Materials; Somerville, NJ, USA). The latter (cresol – novolak positive photoresist that can enable the creation of films 6–20 μm) was carbonized at temperatures in the 600 to 1000 °C range. While a dependence of the resistivity with respect to the thickness of the film was only observed for substrates prepared at lower temperatures (and not on the type of photoresist), they identified slightly different shrinkage patterns during the carbonization process (the shrinkage is generally considered isometric).[56,78] Also using SU-8 as the starting material, De Volder *et al.* implemented a plasma-etching step and was able to fabricate beautiful 3D structures (Fig. 1) that were chemically functionalized and used to measure DNA binding with increased sensitivity.[79] Other modifications of SU-8 include, for example, the possibility of adding a block-copolymer (Pluronic F127) that can act as a porogenic agent.[80]

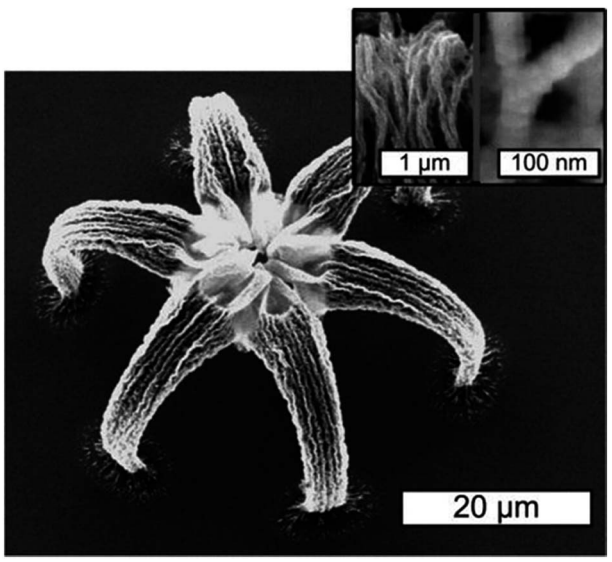

Fig. 1 Example of multilayer processing leading to multiple height 3D CNW microstructure after pyrolysis. Reproduced with permission from ref. 79.

Additional examples of commercial photoresists used for the development of pyrolytic carbon include AZ 4330,[55,65,81] and AZ 9260.[82] In order to fabricate electrodes for electrochemical detection at the microchip scale, Lunte's group utilized AZ 1518 (positive photoresist) and found their performance to be comparable to that of carbon fibers.[83] While not directly applied to an analytical problem, SPR-220-7 (also from MicroChem) has been used to fabricate porous electrodes featuring large surface area.[67] Besides photoresist, a number of materials have been proposed as substrates for pyrolysis. Among those, polyacrylonitrile (spin or solvent casting) has allowed the production of large, conductive films over a wide range of thickness values and over non-planar substrates.[84] An interesting alternative for the fabrication of nanostructured films is the pyrolysis of block copolymers.[85–87] This strategy exploits the periodicity and size of the cavities that are dictated by the MW of each portion of a block co-polymer, the preparation conditions, and the selected solvent.[88] These polymers offer not only the advantage of being commercially available,[86,89] but also their conformation can be fixed *via* cross-linking prior to the pyrolysis.[90] In addition, a variety of conditions can be applied to form thin films by spin-coating.[91] Block copolymers can be also mixed with traditional carbon precursors (resol) and tetraethylorthosilicate (silica precursor) to produce conductive mesoporous carbon-based films. According to the report, composite films with approximately 40 wt% silica displayed a conductivity that was an order of magnitude smaller than the value obtained with a pure carbon mesoporous film, but such conductivity was comparable to typical printed carbon inks used in electrochemical sensing ($\sim$10 S cm^{-1}).[92] Additional methodologies leading to the development and analytical application of carbon substrates modified with cobalt oxide and vanadia[93] or templated with nanoparticles (Fe_3O_4 (ref. 94) or SiO_2 (ref. 95)) have been also reported.

As previously mentioned, initial reports dealing with pyrolysis of cellulose were geared towards applications in the textile industry and a number of reports have demonstrated the possibility to graphitize cellulose from bacteria, algae, animal, and ramie.[51] Using cellulose as substrate, Giuliani *et al.* recently demonstrated the possibility to fabricate electrodes by pyrolysis of a number of paper samples, including printing, filter, photography, and chromatography papers.[35] Considering resistivity measurements and the fragility of the carbonized papers, the imaging card paper, multipurpose printing paper, and 3 MM chromatography paper were further characterized and used as electrochemical transducer for the detection of uric acid. Out the three substrates, 3 MM chromatography paper displayed the best electrochemical performance ($\Delta E_p = 79$ mV, $i_{pa}/i_{pc} = 0.97$, $R_{film} = 2.6 \pm 0.1$ Ω, $R_{ct} = 63 \pm 2$ kΩ) and (upon adsorption of uricase) allowed the development of sensors with good sensitivity (0.225 ± 0.002 mA L $mmol^{-1}$, $R^2 = 0.995$) and LOD (0.004 mmol L^{-1}), figures that were comparable to those obtained with traditional carbon electrodes. In a different approach, Alharthi *et al.* described a versatile and inexpensive procedure to prepare optically transparent carbon electrodes, using proteins as precursors. The proteins were deposited using adsorption (avoiding the need for expensive photoresist or

 This journal is © The Royal Society of Chemistry 2016

Published on 01 April 2016. Downloaded by Clemson University on 15/04/2016 14:03:16.

instrumentation) and pyrolyzed under reductive conditions to form ultrathin, conductive electrodes that allowed the development of a GOx-based biosensor for glucose (LOD = 10 μM).[96] Although not specifically designed towards analytical applications, J. Tour's group reported that the formation of sp^2 clusters (even containing metal-oxide nanoclusters)[97] can be induced by CO_2 laser engraving of polyimide.[98] Although the substrates still required processing in the furnace, this approach could enable the development of patterned electrodes and provide insights about the challenging chemistry involved in the pyrolysis step.

2.4 Structure of the resulting films

One critical aspect in the application of pyrolytic carbon is that these substrates are composed of various forms of carbon ranging from transparent diamond-like structures (sp^3 hybridized) to dark graphite-like clusters (sp^2 hybridized). Because the position and area ratio of the characteristic D (1360 cm^{-1}) and G (1582 cm^{-1}) bands can provide information about the relative abundance of the disordered and graphitic fraction, respectively, Raman spectra are typically obtained as part of the characterization process. As a reference regarding Raman spectra of carbon-based materials, an excellent review by R. McCreery[49] as well as relevant publications by A. Ferrari[99–101] should be consulted. In general, most reports discuss the I_D/I_G ratio, which is correlated with the degree of disorder in the structure. Although a number of attempts have been reported to increase the graphitic fraction of pyrolytic carbon, the resulting structure (properties and subsequent application) seems to be mainly influenced by the composition of the organic precursor and not necessarily by the specific conditions selected for the pyrolysis. For example, pyrolysis of high purity Kapton HN sheets (thickness 0.125 mm; Goodfellow Cambridge Limited, UK) under 10 mL min^{-1} N_2 yielded a I_D/I_G ratio of about 0.7,[102] SU-8 and AR-UL-01 gave almost identical intensity ratios (I_D/I_G = 1.01 and 1.02, respectively),[80,103] AZ nLOF-2070 gave values in the 0.9–1.15 range (depending on the pyrolysis temperature), Pongam seed shells gave values of 0.99 (and 1.01 upon modification with Co_3O_4), and carbon films originated from paper or bovine serum albumin gave a ratio of 1.25 (ref. 35) and 1.26,[96] respectively. Similar values were also reported for ordered carbon films obtained by pyrolysis of covalently attached polyphenylene and polyanthracene layers on silicon substrates.[104] Pyrolysis of a composite made with SU-8 and CNT (pyrolyzed at 600 °C and 10^{-6} Torr) also lead to spectra that resemble the one from graphitic carbon.[105] Probably one of the highest I_D/I_G ratios reported (4.2 ± 0.1) was obtained by pyrolysis of AZ P4330-RS[55] and was correlated with the electrochemical properties observed in the material. With that being said, it is also important to point out that slightly better ratios have been reported for substrates prepared under vacuum treatment, when compared to those prepared in the presence of forming gas[81] and that small differences in the position and intensity of these bands have been reported as a function of the temperature of the pyrolysis step (affecting the graphitization stage).[60] For example, small increases in the crystallinity (I_D/I_G changed from 2.2 to 1.3) of pyrolyzed SU-8 were obtained by adjusting the pyrolysis temperature.[103] In line with the formation mechanism previously described, the I_D/I_G ratio tends to stabilize at about 1000 °C and has not been significantly affected by increasing the dwell time,[56] the pyrolysis time (up to 12 h at 900 °C),[79] or the selected atmosphere (*e.g.* CO_2 activation).[102]

2.5 Thickness, topography, and contact angle

A number of variables can affect the thickness of the resulting film. For the case of spin-coated films, the thickness can be controlled by the spin speed, the viscosity of the selected photoresist, the evaporation rate, and the diffusivity of solute.[91] In all cases, it is worth considering that significant shrinkage (in the wide range of 30 to 90%) is typically observed during the pyrolysis,[56,78] and is especially relevant in the vertical direction – when the substrates are bound to a surface.[48,106] The magnitude of this effect has been linked to the carbon content of the starting material and oxygen content in the furnace's atmosphere.[74,81] One important aspect of these films is the low roughness (in the 0.2–1 nm range[60,65,71,81]) that can be obtained with photoresists. These values can be attributed not only to the uniformity of the layer produced by spin-coating but also to a smoothing process, produced when the uncross-linked photoresist reaches its glass transition temperature (*i.e.* SU-8 = 55 °C). On the contrary, carbon films originated from other carbon sources (such as proteins, structured polymers, or composite materials) render films with larger feature's dimensions.[92,96,107] The presence of these features as well as a rich surface chemistry have opened the door to develop not only solid pre-treatment protocols[4,81,108] but also the attachment of a number of molecules using simple adsorption.[16,109] Although the contact angle of carbon films made by pyrolysis can be significantly affected by surface treatments and the atmosphere selected for the pyrolysis,[110] bare electrodes developed in Ar–H_2 display a contact angle of approximately 80° (hydrophobic).[71,96]

2.6 Optical properties

To rationally select the most suitable electrodes for applications involving optical and electrical measurements, a correct balance between transmittance and resistance should be achieved. Although this relationship is controlled by the thickness of the films,[55] electrodes with thickness values <30 nm, typically display a transmittance above 50%.[60] At a wavelength of 500 nm, for example, films with a thickness of 13 nm and 79 nm displayed transparencies of 47% and 10% and sheet resistances of 1100 Ω cm^{-1} and 210 Ω cm^{-1}, respectively.[65] In general, the absence of active chromophores in the films renders rather featureless spectra, with an absorption band around 250 nm that has been associated with the absorption of light by the disordered graphitic structure.[96] These features are common to other carbon-based nanomaterials (*i.e.* CNT or graphene)[111] and clearly dominate the landscape of optical applications.[65,112]

3. Analytical applications

It is important to point out that electrical contacts to these electrodes must be done after the pyrolysis because common

Published on 01 April 2016. Downloaded by Clemson University on 15/04/2016 14:03:16.

metals used in sputtering process tend to form particles, even when the pyrolysis temperature is kept below their respective bulk melting points.[57] In general, electrical contacts can be made with a drop of silver paint,[35,113] indium wire[106,114] or by sputtering of metals (*i.e.* Ag[112] or Au). The use of standard solder is not recommended to establish a reliable electrical contact.

3.1 Electroanalysis

As pointed out by McCreery, there are at least three phenomena influencing redox activity on carbon surfaces: the resistance of the material, the surface density of electronic states, and the presence of edge plane sites on the electrode surface.[49,115] With the corresponding differences, these features are common to various carbon-based nanomaterials, including graphene.[116–119] In order to understand the role of each contribution, these electrodes are typically characterized by a number of electrochemical techniques, but most commonly cyclic voltammetry and electrochemical impedance spectroscopy. For these experiments, electrochemical couples with well-known behaviors (inner or outer sphere mediators such as $K_4Fe(CN)_6$ or $Ru(NH_3)_6Cl_3$, respectively) are typically used.[120,121] While the former electrochemical couple is probably one of the most used ones and can be utilized to benchmark new materials, readers should be aware that several issues (surface interactions, non-ideality, degradation with time, and sensitivity to light) can potentially affect the results.[115] Most of these experiments are carried out by dissolving the electrochemical couple at a concentration of 1 mM in buffer, KCl, or H_2SO_4. As the electrochemical response of pyrolyzed electrodes is related to their resistivity,[122] the thinner the material, the poorest the response. Therefore, clean cyclic voltammograms (in the −0.4 to +1.2 V range *vs.* $Ag|AgCl|KCl_{sat}$) are typically reported, with peak currents that are proportional to $v^{1/2}$ and peak potentials that largely exceed the ideal separation of 0.059 V/n. As a result, the behavior is often deemed as quasi-reversible or irreversible.[26,55,56] In order to enhance the properties of the material, a number of electrochemical pretreatment steps have been developed,[108] including the simple possibility of activation (electrode cycled in NaOH or H_2SO_4, 0.1 V s^{-1}) to increase the number of functional groups and enhance the hydrophilic character of the surface.[123,124] It is also important to note that recent reports point out the similarities between glassy carbon (activated at +1.8 V *vs.* SCE) and graphene oxide electrodes prepared by Tour or Hummers routes.[125]

Albeit these modifications can provide significant improvements in the electrochemical response, the selectivity of bare electrodes fabricated by pyrolysis is still rather limited. To overcome this shortcoming, square wave anodic voltammetry was utilized to quantify mercury along electrodes fabricated by pyrolysis of AZ 4562 photoresist.[126] In this case, the Hg was deposited (at −0.5 V *vs.* $Ag|AgCl|KCl_{sat}$, for 1800 s) and then stripped during an anodic square wave scan between −0.6 V and 0.2 V (*vs.* $Ag|AgCl|KCl_{sat}$). The stripping peak current observed at −0.45 V was found to be proportional to the concentration of the analyte in the range between 2 ppb and 14 ppb, with a sensitivity of 2.67 μA cm^{-2} ppb^{-1} ($R = 0.996$) and a LOD of 2.4 ± 0.3 ppb. Plain carbon electrodes obtained from pyrolyzed photoresist can be also coupled to separation techniques such as microchip electrophoresis. Following a previous report,[83] Fischer *et al.*[127] demonstrated that microchips fabricated with electrodes from pyrolyzed photoresist films (AZ 1518 or S-1818) displayed better analytical performance than those integrating carbon ink, carbon fibers, or Pd as working electrodes. Specifically, the in-channel configuration (see Fig. 2) displayed a sensitivity of 72 pA μm^{-1} and a LOD of 35 nM, when used to detect dopamine. As a result of limiting band broadening (tailing factor = 0.88) and peak skew (skew factor = 0.75), increases in separation efficiency were observed when mixtures containing dopamine, catechol, and norepinephrine were analyzed.

Although not yet integrated with an analytical method, a procedure to transfer a pyrolyzed polymer onto low thermal tolerance substrates was developed using a layer of either 500 nm SiO_2 or 200 nm of Si_3N_4 as a barrier.[128] According to the report, this process could enable the integration of glassy carbon electrodes to polymeric microfluidic devices (*e.g.* PDMS or PMMA).

One of the drawbacks of using plain carbon electrodes (regardless of how they are fabricated) is that they are prone to surface fouling and can significantly lose their electrochemical response.[8,129,130] Using carbon films obtained from pyrolysis of AZ 4620 photoresist, Brooksby *et al.*[131] investigated the effect of introducing either nitrophenyl (NP) or nitroazobenzene (NAB) groups by an electrochemical process. As expected, cyclic voltammograms showed an irreversible reduction process in the first cycle (formation of a grafted layer on the electrode surface) that passivized the surface and blocked all subsequent electrochemical processes. Accordingly, the surface coverage for a NP monolayer was estimated as $(2.5 \pm 0.5) \times 10^{-10}$ mol cm^{-2}, and corresponds to approximately 21% of an ideal close-packed monolayer. Similar results were also reported by Leroux *et al.*[132] and Nasraoui,[133] who investigated the electrochemical effects of depositing dense layers of ethynyl-aryl functionalized using azidomethylferrocene or aliphatic primary amines containing a carboxylic or ester group at the opposite end, respectively. While removing these tightly bound layers from the surface of conventional carbon electrodes can be accomplished by mechanical polishing, sonication, heat, electrochemical, and/or solvent treatments; the thickness and topography of thin carbon films fabricated by pyrolysis requires the development of specific strategies. Among them, Gross *et al.*[134] described a time- and cost-effective procedure to regenerate electrochemical activity of electrodes fabricated from pyrolysis of AZ 4620 and then coated with an insulating film, attached *via* electrografting from aryldiazonium salt solutions. In the report, a simple heating treatment (at 545 °C for 30 min) was sufficient to recover well-defined peak currents with slightly larger current values and a peak-to-peak potential separation smaller than the electrode performance prior to the modification and heat treatment. Although applied to carbon fibers, Takmakov *et al.*[135] described a procedure that constantly renews the surface of a carbon microelectrode using periodic triangle voltage excursions to an extended anodic potential at a scan rate of 400 V s^{-1}.

 This journal is © The Royal Society of Chemistry 2016

Published on 01 April 2016. Downloaded by Clemson University on 15/04/2016 14:03:16.

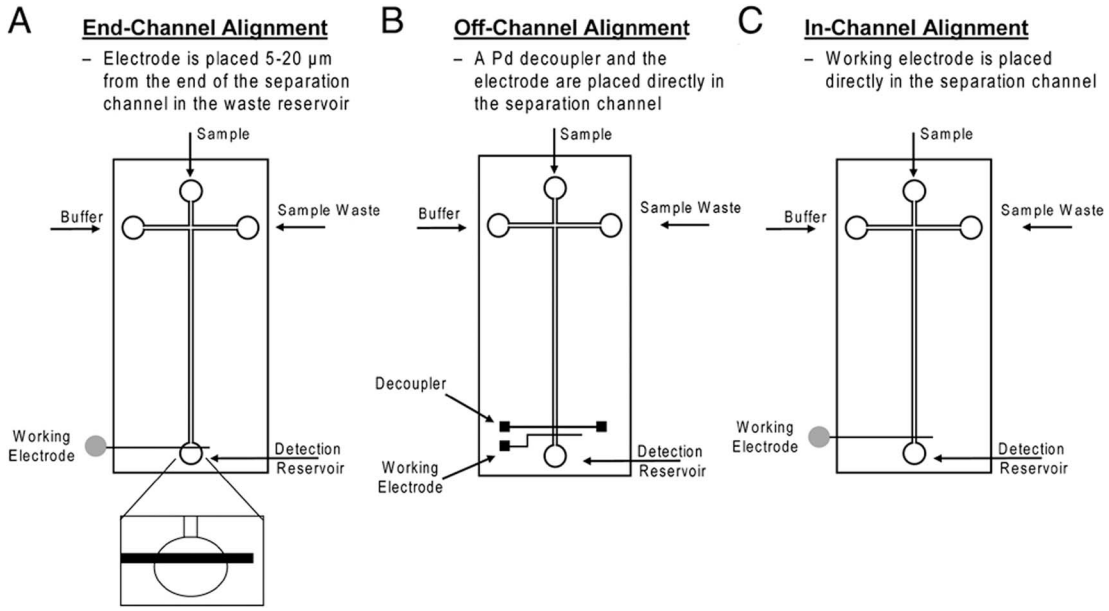

Fig. 2 Schematic diagram of different electrode alignments for microchips electrophoresis with electrochemical detection: (A) end-channel electrode alignment, (B) off-channel electrode alignment, and (C) in-channel electrode alignment. Reprinted with permission from ref. 127.

The second strategy to improve the electrochemical detection of molecules using electrodes developed by pyrolysis is the modification of the material itself (composites). As examples of this approach, electrodes were fabricated by pyrolysis of Pongam seed shells impregnated with cobalt oxide nanoparticles (2–10 nm, PSAC/Co_3O_4).[93] Upon characterization, the PSAC/Co_3O_4-modified electrode was employed to develop a high performance non-enzymatic glucose sensor and a supercapacitor. Remarkably, the fabricated glucose sensor exhibited an ultrahigh sensitivity of 34.2 mA mM^{-1} cm^{-2}, a very low LOD (21 nM), and long-term durability. Along the same lines, Duran *et al.*[113] recently developed a procedure to generate CuNPs on the structure of pyrolyzed paper. The methodology is based on the pyrolysis (1000 °C under a mixture of 95% Ar–5% H_2 for 1 h) of paper strips modified with a saturated solution of $CuSO_4$ (1.3 M), which yields abundant CuNPs on the surface of carbonized cellulose fibers (Fig. 3).

After being characterized by a combination of different techniques (resistivity, microscopy, Raman spectroscopy, cyclic voltammetry, and electrochemical impedance spectroscopy) these CuNPs-modified carbon electrodes (CuNPs@CE) were used for non-enzymatic amperometric detection of glucose at +0.65 V (*vs.* Ag|AgCl|KCl_{sat}). The analytical performance of the glucose sensor displayed a linear range up to 3 mM with a sensitivity of 460 ± 8 μA cm^{-2} mM^{-1} (R^2 = 0.998), LOD = 5 μM, and LOQ = 17 μM and negligible response to common interferences. Similarly, films containing multilayered graphene (MLG) and gold nanoparticles (AuNPs-MLG) were described by Ilanchezhiyan *et al.*[136] In this case, a mixture of $HAuCl_4$ and photoresist S-1813 G was spin-coated and pyrolyzed using a rapid thermal annealing system (RTA). Raman spectroscopy demonstrated the presence of graphene layers by revealing the sp^2 vibration of carbon atoms in the 2D hexagonal lattice (G band) and the double-resonance process (2D band) in the MLG (blank carbon films). AuNPs were found to be homogeneously attached over the graphene surface and without significant aggregation, configuration that resulted in a decrease in sheet resistance from 1100 Ω sq^{-1} (non-modified

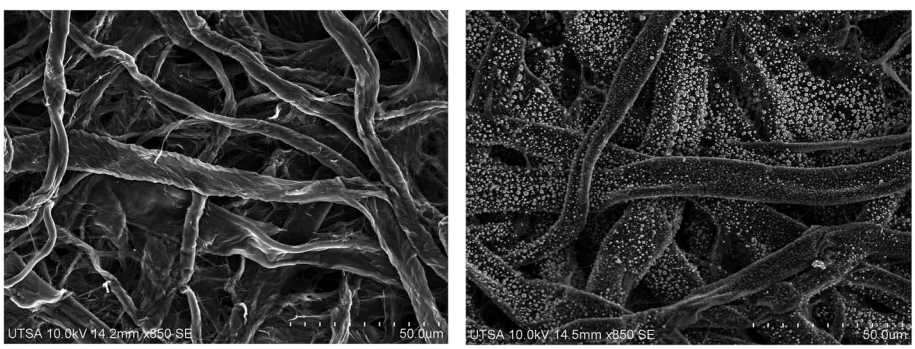

Fig. 3 SEM images of pyrolyzed paper fibers in absence (left) and presence (right) of CuNPs. Reprinted with permission from ref. 113.

Published on 01 April 2016. Downloaded by Clemson University on 15/04/2016 14:03:16.

carbon films) to 459 Ω sq^{-1} (AuNPs-modified carbon films). Authors associated this observation with a systematic downward shift noted in XPS experiments and concluded that a charge transfer process could be taking place between MLG and Au.

It is important to mention that the surface of carbon substrates features a number of chemical groups that can be used to tailor the analytical properties of the resulting detection electrodes. Therefore, a third alternative to improve the performance of these electrodes is to modify the electrode's surface. Under this category it is worth mentioning the possibility of using bismuth to modify the surface of carbon electrodes derived from pyrolyzed S-1813SP5 photoresist films.[137] In this case, electrodes were used for simultaneous determination of Pb(II), Cd(II), and Zn(II) in aqueous solutions by stripping analysis using square wave voltammetry (E_{step} = 0.025 V, E_{pulse} = 0.080 V *vs.* Ag|AgCl|KCl_{sat}, and frequency 25 Hz). After optimizing the Bi(III) concentration on the modification procedure, three well-defined peaks corresponding to Pb(II) (~−0.60 V), Cd(II) (~−0.85 V), and Zn(II) (~−1.2 V) were obtained, with linear responses in the 10–90 nM and calculated LODs in the 18–10 nM for all tested analytes. Rehacek *et al.* reported that pyrolyzed SU-8 can also be modified with the same procedure and the performance of the electrodes further improved by coating the electrodes with Nafion.[138] The analytical sensitivities of Nafion-coated BiFE towards Pb(II) and Cd(II) (398 and 539 μA μM^{-1}, respectively) were twice higher than those observed for bare BiFE electrodes (200 and 253 μA μM^{-1}, respectively) but only slightly improved for Zn(II) (170 μA μM^{-1}). The resulting LODs were calculated as 3 nM, 6 nM, and 24 nM for Pb(II), Cd(II), and Zn(II), respectively. Other analytical applications of bismuth-modified electrodes include the determination of trace levels of Cd(II) and Pb(II),[56] nickel,[139] and chromium.[68,140] Xiao *et al.*[141] deposited Pd nanoparticles in nanoporous carbon electrodes fabricated by pyrolysis of substrates patterned using interference lithography. To obtain the carbon electrodes, a silicon wafer was sequentially coated with an anti-reflection coating (ICON-7; Brewer Science, Roll, MO, USA), a thin layer of negative tone NR7-100P (used as an adhesion layer) and a 6 μm layer of NR7-6000P. The photoresist was patterned using a Q-switched Nd:YAG laser, pyrolyzed, rinsed with isopropanol/water, and electrochemically modified with Pd. As shown in Fig. 4, porous electrodes with nanoparticles varying in shape, density, and size were obtained as a function of the exposure time and the applied potential.

Electrodes fabricated by applying −0.65 V during 100 s rendered flower-like nanocrystals and were used to examine the catalytic activity towards glucose. The presented Pd-modified electrode showed higher current density (2.27 mA cm^{-2} at −0.03 V) than glassy carbon electrodes (0.30 mA cm^{-2} at −0.23 V) modified in the same way and allowed the fast (response time < 5 s) amperometric analysis of glucose (−0.2 V) in the 1–30 mM range and a LOD = 10 μM. Depositing Ag–Pt nanoparticles onto porous-structured polyacrylonitrile (PAN) nanofibers (pPAN) has also allowed the defection of dopamine (linear range 10–500 μM and a LOD of 0.11 μM) in the presence of uric acid and ascorbic acid.[142]

Another solution to improve the electrochemical activity of electrodes fabricated by pyrolysis is to coat their surface with traditional carbon-based nanomaterials. As an example of this approach, Ligia Moretto's group performed the electrochemical detection of *o*-toluidine (a carcinogenic organic compound employed in the synthesis of azo-dyes) using electrodes modified with an spray containing CNT (0.25 mg mL^{-1}).[143] Optimum results were obtained by depositing 3 layers of the CNT suspension dosed by a syringe pump at 2 mL min^{-1} and sprayed by a 3 bar air flux, from a distance of 9 cm, and keeping the substrates at 120 °C to ensure solvent evaporation. In this case, a sensitivity of 6.49 μA cm^{-2} ppm^{-1}, a LOD of 0.089 ppm, and a LOQ of 0.270 ppm were reported. In a similar approach, a commercial carbon-based paper (Toray Industries, Inc.; Tokyo, Japan) was modified by the electrospinning of polyacrylonitrile fibers directly onto a polyacrylonitrile-coated substrate followed by carbonization at 1200 °C.[144] This substrates were used to detect dopamine in one of the widest ranges reported to date (0.2 μM–0.7 M) and with a calculated LOD of 0.08 μM.

Not only solution-based methods have been applied to modify the surface of glassy carbon electrodes. As an example, Yang *et al.* used UV radiation (253.7 nm) and ammonia to selectively modify carbon 3D structures (pillars) fabricated from pyrolyzed SU-8.[145] This direct amination process required about 4 h and enabled the attachment of ss-DNA to the top surface of the carbon substrates. Aiming to optimize the surface functionalization conditions for covalent binding of bioreceptors, a comparison of different oxidation pretreatments (vacuum ultraviolet, electrochemical activation, oxygen reactive ion etching, and ultraviolet/ozone) was also recently published.[124] Similarly, films derived from positive AZ 4620 photoresist were iodinated by plasma exposure with iodine and then allowed to react with alkene (undecylenic acid and S-undec-10-enyl-2,2,2-trifluoroethanethioate, C_{11}-S-TFA) and alkyne (1,8-nonadiyne) compounds for 12–16 h under light exposure (λ = 514 nm). Although in both cases the electrochemical data was compatible with the formation of a densely packed layer formed at the interface (in line with previously discussed reports[131–134]), removal of the protective TFA from the alkene-modified films revealed thiol moieties which were used to bind gold nanoparticles. On the other hand, the 1,8-nonadiyne-modified surface was used to attach an azide derived from tetra(ethylene glycol) using "click" chemistry, generating hydrophobic surfaces with potential applications in the control of surface adhesion of biomolecules.

3.2 Development of biosensors

Beyond the biosensing applications of previously discussed substrates,[35,82,96,141] a number of research groups have presented biosensors based on carbon substrates developed by pyrolysis.[146] As specific examples, carbon fibers fabricated by the pyrolysis of electrospun polyacrylonitrile fibers were cut into disks and modified with glucose oxidase using a solution containing Nafion. The resulting electrodes were operated in PBS (pH = 7.0) with an applied electrode potential of −0.42 V and

 This journal is © The Royal Society of Chemistry 2016

Published on 01 April 2016. Downloaded by Clemson University on 15/04/2016 14:03:16.

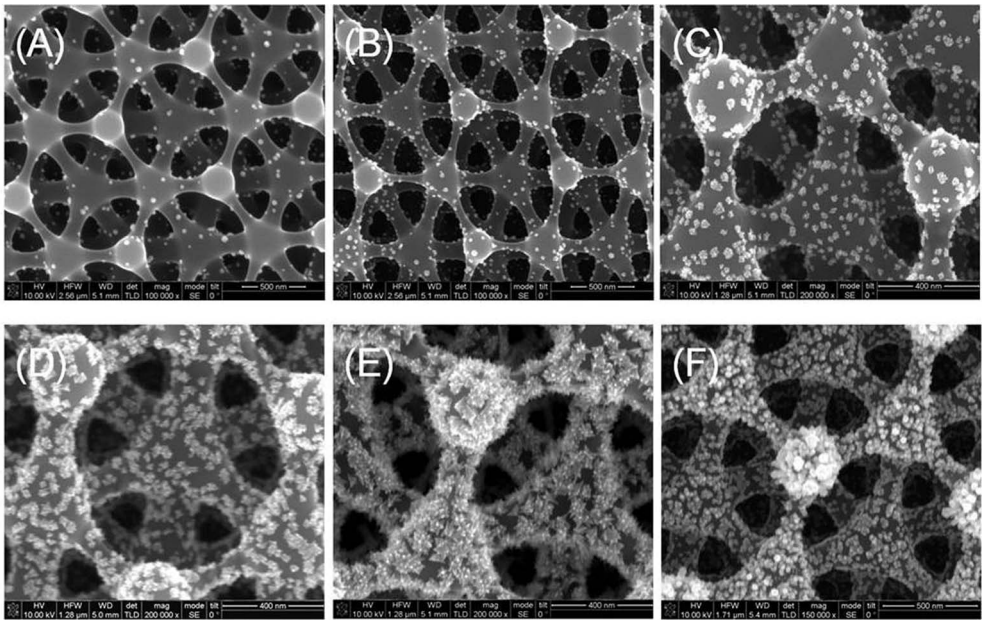

Fig. 4 SEM images of Pd-modified 3D porous carbon electrodes. (A–E) Deposition at −0.65 V for 5, 10, 20, 50, and 100 s. (F) Deposition at −0.45 V for 100 s. Reprinted with permission from ref. 141.

yielded a linear response range from 0.2 to 1.2 mM ($R = 0.998$) and a LOD of 60 μM.[147] Another example of the great potential of 3D carbon electrodes developed by pyrolysis of SU-8 is the detection of a platelet-derived growth factor (PDGF-BB) oncoprotein.[148] In this case, the detection mechanism is based on the release of fluorophore (TOTO intercalating dye) from the target binding aptamer's stem structure when it captures PDGF, showing near linear relationship between the relative fluorescence difference and protein concentration even in the sub-nanomolar range with a detection limit of 5 pmol. As shown in Fig. 5, similar structures were later modified *via* vacuum and UV light to introduce –COOH groups and applied for the detection of a HIV peptide down to 50 pM levels, which is well-within the useful clinical range.[149]

Taking advantage of their high affinity for carbon surfaces,[96] a number of biomolecules have been immobilized on the surface of various carbon substrates *via* adsorption.[150–152] Additionally, and because adsorption is a step required for most immobilization processes, much attention has been given to this process to maximize the overall activity of the biosensor.[109] The only caveat to take advantage of this possibility and maximize the activity of the adsorbed enzyme is the necessity to gain a detailed description of the driving forces and consequences of the interaction process. In this regard, carbon electrodes

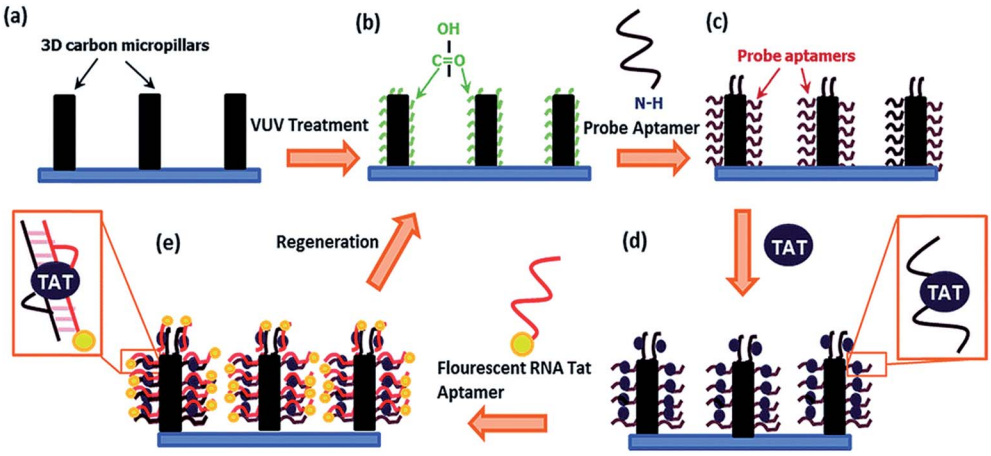

Fig. 5 Schematic illustration of the detection of HIV-TAT peptide using RNA aptamers on 3D carbon microarrays platform; (a) bare carbon micropillar platform, (b) surface functionalization of the carbon surface using vacuum and UV light pretreatment, (c) covalent immobilization of the probe RNA aptamer, (d) intercalating the HIV-TAT peptide to the probe aptamer (e) binding of the fluorescence labelled RNA^{Tat} aptamer with the probe RNA aptamer forming a duplex with Tat peptide in between. Reproduced with permission from ref. 149.

Published on 01 April 2016. Downloaded by Clemson University on 15/04/2016 14:03:16.

obtained from pyrolysis of photoresist (AZ 4330-RS) present a unique balance of optical, electrical, and chemical properties[55] to perform such studies in real time and under a variety of experimental conditions. For the cases described by our group, and performed by spectroscopic ellipsometry (related information available elsewhere[153,154]), electrodes with a thickness of about 20 nm were considered most appropriate and prepared using a 60% dilution of the photoresist in propylene glycol monomethyl ether acetate (T = 43%, and R = 631 Ω). The unique aspect of these electrodes is that they enabled investigating the effect of electric potential applied during the adsorption process of various proteins relevant to analytical applications.[55,155–157] As a summary of those experiments, it can be concluded that unlike adsorption at open-circuit potential, where a combination of electrostatic and hydrophobic forces typically leads to the formation of a monolayer of enzymes with different final activity, the application of potential (up to the corresponding peak potential[156]) can polarize the incoming proteins and induce the deposition of multiple layers of proteins. For the specific case of glucose oxidase, this potential-induced phenomenon can result in carbon substrates with a catalytic activity that is twice as large as the activity of electrodes prepared at open-circuit potential.

3.3 Dielectrophoresis

Although metallic electrodes have been traditionally used to develop devices for dielectrophoresis, few groups have noted that glass-like carbon electrodes offer a wider electrochemical stability window (limited electrolysis) than gold and platinum, are not limited to planar geometries, and can be fabricated at relatively low-cost. Martinez-Duarte *et al.*[158] developed a carbon-electrode dielectrophoresis (carbonDEP) array as an alternative to the traditional DEP techniques. SU-8 negative photoresist was used as carbon precursor and UV-photolithography utilized to pattern arrays with high aspect ratios on transparent fused-silica substrates. After characterizing the processing parameters (spin coating, soft and hard bake, UV exposure, *etc.*), the most appropriate conditions were selected to develop applications including positioning, filtering, and sorting of latex particles, *Drosophila melanogaster* cells,[159] and *Saccharomyces cerevisiae* cells.[160] An experimental and theoretical study was also performed using 3D electrodes contained in a microfluidic channel for DEP manipulation of λ-DNA (48.5 kbp) by Martinez-Duarte *et al.*[114] The structure of the array consisted of planar interdigitated fingers connected to large connection pads, and then 3D electrodes of 95 ± 5 μm in height were fabricated on top of each interdigitated fingers. Experimental results demonstrated that DNA can be manipulated and trapped with these carbon electrodes, yielding a ~20-fold enrichment of 48.5 λ-DNA (according to the theoretical model presented). CarbonDEP has also been demonstrated in an assay to concentrate and purify yeast populations to improve the sensitivity of a standard PCR protocol by increasing the number of targets and eliminating a common polymerase inhibitor.[161] A similar assay was also used to concentrate *Mycobacterium smegmatis* cells surviving exposure to antibiotics, towards providing a tool to facilitate the study of persistent bacterial populations in tuberculosis.[162] These 3D carbon electrode arrays were also used to implement electrical cell lysis of both yeast cells and T-cell acute lymphoblastic leukemia (RPMI8402) cells. The use of dense electrode arrays allowed for high throughput lysis at flow rates as high as 100 μl min^{-1}.[163]

3.4 Solid phases for separations

In general, the interaction of glassy carbon substrates with analytes is determined by a combination of hydrophobic and electrostatic forces as well as their potential to interact *via* π–π stacking.[164] In order to preconcentrate pesticides, films of polydopamine were prepared and in alkaline media over stainless-steel fibers. These fibers provided a simple way to obtain enrichment factors in the 102–757 range.[165] Zewe *et al.*[166] used glassy carbon fibers obtained by electrospinning of SU-8 2100 photoresist onto stainless steel wires and subsequent pyrolysis (at 400, 600, and 800 °C) for solid-phase microextraction (SPME) of nonpolar (benzene, toluene, ethylbenzene, and *o*-xylene) and polar (phenol, 4-chlorophenol, and 4-nitrophenol) compounds. After pyrolysis (400–600 °C range), the carbon nanofibers showed an increased porosity and surface area, trend that was reversed for samples obtained at 800 °C. Additionally, micropores (with widths of 20 Å or less) represented about 20% of the porosity and the average pore diameter decreased accordingly the increment of processing temperature. Although the fibers obtained at 600 °C exhibited the higher extraction efficiency for nonpolar compounds, the distribution coefficient for benzene demonstrated increasing interactions with the carbon fibers as the processing temperature increased. Similarly, the development and application of electrospun glassy carbon nanofibers for ultra-thin layer chromatography (UTLC) was reported by Clark *et al.*[167] In this case, carbon nanofibers obtained by the electrospinning and pyrolysis of SU-8 2100 photoresist were used as stationary phase. Three different temperatures (600, 800, and 1000 °C) were used to pyrolyzed the samples. In line with the shrinkage phenomenon previously discussed, carbon fibers with larger diameters were obtained at 600 °C and displayed the fastest mobile phase velocities, the biggest effective pore radius, and the highest hydrophilic character. These parameters tend to decrease as the carbonization temperature increased, and allowed the separation of a mixture of sulforhodamine 640, rhodamine 610 perchlorate, and pyrromethene 597. More recently, C. Lucy's group described the possibility of modifying commercial porous graphitic carbon particles with carboxylic acid groups and their use as stationary phase for hydrophilic interaction liquid chromatography.[168] Taking advantage of its electrical properties, one of the most interesting applications of carbon in separation science was the development of electrochemically modulated liquid chromatography.[169,170] In this separation technique, the selectivity of the column can be dynamically adjusted by changing the potential applied to a column made of glassy carbon. While this approach has not received all the attention its probably deserves, Yakes[171] and Barrow[172] have developed methods for the separation of triazines and a mixture of acrylamide and

 This journal is © The Royal Society of Chemistry 2016

Published on 01 April 2016. Downloaded by Clemson University on 15/04/2016 14:03:16.

hydrocortisone, respectively. The latter report also serves as example of the potential of these columns to be patterned into a microfluidic-type device.

4. Conclusions and future directions

Considering the number of issues that can affect the response of traditional electrode materials (both metallic and carbon-based[173]), the increasing interest for the development of glassy carbon from pyrolysis of various solid materials is clearly justified. Glassy carbon substrates (defined as those fabricated from pyrolysis of pre-deposited, non-volatile substrates) offer unique properties that can be finely tuned to meet the requirements of a diverse number of analytical methodologies including those based on optical, electrochemical, or chromatographic principles. At this point, the mechanism involved in the pyrolysis step is fairly well established and renders substrates that progressively release compounds with low-MW, non-carbon elements (oxygen and hydrogen), compact, and crosslink; therefore increasing the conductivity and hydrophobicity of the resulting material. While the general properties of carbon-based substrates can be slightly adjusted by adequately selecting the starting material and the deposition conditions (which in turn affects the roughness, thickness, transparency, and resistivity), the structural composition of the resulting films (graphitic *vs.* disordered fraction) does not seem to respond to any of the variables involved in the pyrolysis. To the best of our knowledge, only few reports have described the potential role of metals in a so-called local-CVD process[57] that could lead to significant increases of the graphitic fraction in these substrates *via* a catalyzed mechanism. In this regard it should be noted that while copper foil seems to facilitate the formation of graphene,[72,98] the pyrolysis of organic materials containing metallic ions (*e.g.* copper-impregnated paper[113] or metal–organic frameworks[174]) has not yet lead to significant improvements in the graphitic fraction in the resulting composites. Another area where these materials could have a large impact in the near future is the development of novel separation phases[175–177] and multifunctional materials, where the electrical and/or optical properties can be adjusted in response to external stimuli. In summary, the presented results show a number of examples that highlight the advantages of carbon substrates prepared by pyrolysis, provide a glimpse of the intriguing complexity of the chemical reactions occurring at high temperatures, and indicate that that many more applications are expected to further enrich the body of literature in this field.

Acknowledgements

The authors gratefully acknowledge the financial support provided by Clemson University.

References

1 L. Gorton, *Electroanalysis*, 1995, **7**, 23.
2 I. Svancara, K. Vytras, K. Kalcher, A. Walcarius and J. Wang, *Electroanalysis*, 2009, **21**, 7.
3 W. E. V. d. Linden and J. W. Dieker, *Anal. Chim. Acta*, 1980, **119**, 1.
4 A. Dekanski, J. Stevanović, R. Stevanović, B. Ž. Nikolić and V. M. Jovanović, *Carbon*, 2001, **39**, 1195.
5 K. Pecková, J. Musilová and J. Barek, *Crit. Rev. Anal. Chem.*, 2009, **39**, 148.
6 J. H. T. Luong, K. B. Male and J. D. Glennon, *Analyst*, 2009, **134**, 1965.
7 A. N. Patel, M. G. Collignon, M. A. O'Connell, W. O. Y. Hung, K. McKelvey, J. V. Macpherson and P. R. Unwin, *J. Am. Chem. Soc.*, 2012, **134**, 20117.
8 Y. Ding, A. Ayon and C. D. García, *Anal. Chim. Acta*, 2007, **584**, 244.
9 M. Trojanowicz, *TrAC, Trends Anal. Chem.*, 2006, **25**, 480.
10 C. Yang, M. E. Denno, P. Pyakurel and B. J. Venton, *Anal. Chim. Acta*, 2015, **887**, 17.
11 S. Guo and S. Dong, *Chem. Soc. Rev.*, 2011, **40**, 2644.
12 K. Toda, R. Furue and S. Hayami, *Anal. Chim. Acta*, 2015, **878**, 43.
13 S. Benítez-Martínez and M. Valcárcel, *TrAC, Trends Anal. Chem.*, 2015, **72**, 93.
14 X. T. Zheng, A. Ananthanarayanan, K. Q. Luo and P. Chen, *Small*, 2015, **11**, 1620.
15 K. Scida, P. W. Stege, G. Haby, G. A. Messina and C. D. García, *Anal. Chim. Acta*, 2011, **691**, 6.
16 B.-T. Zhang, X. Zheng, H.-F. Li and J.-M. Lin, *Anal. Chim. Acta*, 2013, **784**, 1.
17 A. Speltini, D. Merli and A. Profumo, *Anal. Chim. Acta*, 2013, **783**, 1.
18 P. R. Unwin, *Faraday Discuss.*, 2014, **172**, 521.
19 K. Kinoshita, *Carbon: electrochemical and physicochemical properties*, Wiley, 1988.
20 R. McCreery, A. Bergren, A. Morteza-Najarian, S. Y. Sayed and H. Yan, *Faraday Discuss.*, 2014, **172**, 9.
21 E. Fitzer, K.-H. Kochling, H. P. Boehm and H. Marsh, *Pure Appl. Chem.*, 2009, **67**, 473.
22 G. L. Dong and K. J. Hüttinger, *Carbon*, 2002, **40**, 2515.
23 A. Li, S. Zhang, B. Reznik, S. Lichtenberg, G. Schoch and O. Deutschmann, *Proc. Combust. Inst.*, 2011, **33**, 1843.
24 J. R. Fincke, R. P. Anderson, T. A. Hyde and B. A. Detering, *Ind. Eng. Chem. Res.*, 2002, **41**, 1425.
25 Y.-Z. Chen, H. Medina, H.-W. Tsai, Y.-C. Wang, Y.-T. Yen, A. Manikandan and Y.-L. Chueh, *Chem. Mater.*, 2015, **27**, 1646.
26 N. McEvoy, N. Peltekis, S. Kumar, E. Rezvani, H. Nolan, G. P. Keeley, W. J. Blau and G. S. Duesberg, *Carbon*, 2012, **50**, 1216.
27 Y. Zhang, L. Zhang and C. Zhou, *Acc. Chem. Res.*, 2013, **46**, 2329.
28 W. J. Blaedel and G. A. Mabbott, *Anal. Chem.*, 1978, **50**, 933.
29 K. B. Teo, C. Singh, M. Chhowalla and W. I. Milne, *Catalytic Synthesis of Carbon Nanotubes and Nanofibers, Encyclopedia of Nanoscience and Nanotechnology*, 2003, vol. X, American Scientific Publisher, Stevenson, CA 91381, USA, pp. 1–22.
30 M. Kumar and Y. Ando, *J. Nanosci. Nanotechnol.*, 2010, **10**, 3739.

Published on 01 April 2016. Downloaded by Clemson University on 15/04/2016 14:03:16.

31 M. Mojica, J. A. Alonso and F. Méndez, *J. Phys. Org. Chem.*, 2013, **26**, 526.
32 V. Georgakilas, J. A. Perman, J. Tucek and R. Zboril, *Chem. Rev.*, 2015, **115**, 4744.
33 N. Yang, X. Chen, T. Ren, P. Zhang and D. Yang, *Sens. Actuators, B*, 2015, **207**, 690.
34 S. E. Skrabalak and K. S. Suslick, *J. Am. Chem. Soc.*, 2006, **128**, 12642.
35 J. G. Giuliani, T. E. Benavidez, G. M. Duran, E. Vinogradova, A. Rios and C. D. Garcia, *J. Electroanal. Chem.*, 2016, **765**, 8.
36 E. Weintraub and L. B. Miller, Google Patents, 1915, *Patent US1156509 A*.
37 H. W. Davidson, *Nucl. Sci. Eng.*, 1962, **7**, 159.
38 E. Fitzer, W. Schaefer and S. Yamada, *Carbon*, 1969, **7**, 643.
39 T. Noda and M. Inagaki, *Bull. Chem. Soc. Jpn.*, 1964, **37**, 1534.
40 G. M. Jenkins and K. Kawamura, *Nature*, 1971, **231**, 175.
41 B. O'Malley, I. Snook and D. McCulloch, *Phys. Rev. B: Condens. Matter Mater. Phys.*, 1998, **57**, 14148.
42 A. K. Burnham, X. Zhou and L. J. Broadbelt, *Energy Fuels*, 2015, **29**, 2906.
43 A. G. W. Bradbury, Y. Sakai and F. Shafizadeh, *J. Appl. Polym. Sci.*, 1979, **23**, 3271.
44 M. M. Tang and R. Bacon, *Carbon*, 1964, **2**, 211.
45 T. Kyotani, *Carbon*, 2000, **38**, 269.
46 J. Kim, X. Song, K. Kinoshita, M. Madou and R. White, *J. Electrochem. Soc.*, 1998, **145**, 2314.
47 K. Kinoshita, X. Song, J. Kim and M. Inaba, *J. Power Sources*, 1999, **81–82**, 170.
48 P. Varun, K. Hiroshi and C. Wang, *J. Micromech. Microeng.*, 2012, **22**, 045024.
49 R. L. McCreery, *Chem. Rev.*, 2008, **108**, 2646.
50 J. Goma and M. Oberlin, *Thin Solid Films*, 1980, **65**, 221.
51 D.-Y. Kim, Y. Nishiyama, M. Wada and S. Kuga, *Carbon*, 2001, **39**, 1051.
52 O. J. A. Schueller, S. T. Brittain and G. M. Whitesides, *Adv. Mater.*, 1997, **9**, 477.
53 A. Ponrouch, A. R. Goñi and M. R. Palacín, *Electrochem. Commun.*, 2013, **27**, 85.
54 R. Taylor, G. J. Langley, H. W. Kroto and D. R. M. Walton, *Nature*, 1993, **366**, 728.
55 T. E. Benavidez and C. D. Garcia, *Electrophoresis*, 2013, **34**, 1998.
56 A. Mardegan, R. Kamath, S. Sharma, P. Scopece, P. Ugo and M. Madou, *J. Electrochem. Soc.*, 2013, **160**, B132.
57 C. Wang, R. Zaouk and M. Madou, *Carbon*, 2006, **44**, 3073.
58 M. Frenklach, in *Preprints of Papers Presented at the 197th ACS National Meeting*, ACS Division of Fuel Chemistry, Dallas, TX, 1989, vol. 34, p. 451.
59 N. Sano, H. Akazawa, T. Kikuchi and T. Kanki, *Carbon*, 2003, **41**, 2159.
60 M. Schreiber, T. Lutz, G. P. Keeley, S. Kumar, M. Boese, S. Krishnamurthy and G. S. Duesberg, *Appl. Surf. Sci.*, 2010, **256**, 6186.
61 K. L. Cashdollar, I. A. Zlochower, G. M. Green, R. A. Thomas and M. Hertzberg, *J. Loss Prev. Process Ind.*, 2000, **13**, 327.
62 Y. Saito, K. Sato, H. Tanaka, K. Fujita and S. Matuda, *J. Mater. Sci.*, 1988, **23**, 842.
63 K. Hata, D. N. Futaba, K. Mizuno, T. Namai, M. Yumura and S. Iijima, *Science*, 2004, **306**, 1362.
64 Sigma-Aldrich Bulletin 898C, 2000-accessed March 2016.
65 S. Donner, H.-W. Li, E. S. Yeung and M. D. Porter, *Anal. Chem.*, 2006, **78**, 2816.
66 M. Silvestrini, A. Mardegan, R. Kamath, M. Madou, L. M. Moretto, S. Passamonti, P. Scopece and P. Ugo, *Electrochim. Acta*, 2014, **147**, 401.
67 S. Wang, B. Hsia, C. Carraro and R. Maboudian, *J. Mater. Chem.*, 2014, **2**, 7997.
68 A. Mardegan, M. Cettolin, R. Kamath, V. Vascotto, A. M. Stortini, P. Ugo, P. Scopece, M. Madou and L. M. Moretto, *Electroanalysis*, 2015, **27**, 128.
69 F. J. del Campo, P. Godignon, L. Aldous, E. Pausas, M. Sarrión, M. Zabala, R. Prehn and R. G. Compton, *J. Electrochem. Soc.*, 2011, **158**, H63.
70 H. Kimura, J. Goto, S. Yasuda, S. Sakurai, M. Yumura, D. N. Futaba and K. Hata, *Sci. Rep.*, 2013, **3**, 3334.
71 H. Lee, R. Rajagopalan, J. Robinson and C. G. Pantano, *ACS Appl. Mater. Interfaces*, 2009, **1**, 927.
72 G. Ruan, Z. Sun, Z. Peng and J. M. Tour, *ACS Nano*, 2011, **5**, 7601.
73 R. Madhu, V. Veeramani and S.-M. Chen, *Sci. Rep.*, 2014, **4**, 4679.
74 A. Singh, J. Jayaram, M. Madou and S. Akbar, *J. Electrochem. Soc.*, 2002, **149**, E78.
75 J. I. Heo, D. S. Shim, G. T. Teixidor, S. Oh, M. J. Madou and H. Shin, *J. Electrochem. Soc.*, 2011, **158**, J76.
76 F. Liu, G. Kolesov and B. A. Parkinson, *Anal. Chem.*, 2014, **86**, 7391.
77 Y. Lim, J.-I. Heo and H. Shin, *Sens. Actuators, B*, 2014, **192**, 796.
78 B. Y. Park, L. Taherabadi, C. Wang, J. Zoval and M. J. Madou, *J. Electrochem. Soc.*, 2005, **152**, J136.
79 M. F. L. De Volder, R. Vansweevelt, P. Wagner, D. Reynaerts, C. Van Hoof and A. J. Hart, *ACS Nano*, 2011, **5**, 6593.
80 V. Penmatsa, J.-H. Yang, Y. Yu and C. Wang, *Carbon*, 2010, **48**, 4109.
81 S. Ranganathan, R. McCreery, S. M. Majji and M. Madou, *J. Electrochem. Soc.*, 2000, **147**, 277.
82 J. A. Lee, S. Hwang, J. Kwak, S. I. Park, S. S. Lee and K.-C. Lee, *Sens. Actuators, B*, 2008, **129**, 372.
83 D. J. Fischer, W. R. Vandaveer, R. J. Grigsby and S. M. Lunte, *Electroanalysis*, 2005, **17**, 1153.
84 C. L. Renschler, A. P. Sylwester and L. V. Salgado, *J. Mater. Res.*, 1989, **4**, 452.
85 S. Park, J.-Y. Wang, B. Kim, J. Xu and T. P. Russell, *ACS Nano*, 2008, **2**, 766.
86 D. A. Rider, K. Liu, J.-C. Eloi, L. Vanderark, L. Yang, J.-Y. Wang, D. Grozea, Z.-H. Lu, T. P. Russell and I. Manners, *ACS Nano*, 2008, **2**, 263.
87 Y. Deng, C. Liu, T. Yu, F. Liu, F. Zhang, Y. Wan, L. Zhang, C. Wang, B. Tu, P. A. Webley, H. Wang and D. Zhao, *Chem. Mater.*, 2007, **19**, 3271.

 This journal is © The Royal Society of Chemistry 2016

Published on 01 April 2016. Downloaded by Clemson University on 15/04/2016 14:03:16.

88 S. Krishnamoorthy, C. Hinderling and H. Heinzelmann, *Mater. Today*, 2006, **9**, 40.
89 X. Deng, J. M. Buriak, P.-X. Dai, L.-J. Wan and D. Wang, *Chem. Commun.*, 2012, **48**, 9741.
90 D.-Y. Kang, C. Kim, G. Park and J. H. Moon, *Sci. Rep.*, 2015, **5**, 18185.
91 K. Norrman, A. Ghanbari-Siahkali and N. B. Larsen, *Annu. Rep. Prog. Chem., Sect. C: Phys. Chem.*, 2005, **101**, 174.
92 L. Song, D. Feng, C. G. Campbell, D. Gu, A. M. Forster, K. G. Yager, N. Fredin, H.-J. Lee, R. L. Jones, D. Zhao and B. D. Vogt, *J. Mater. Chem.*, 2010, **20**, 1691.
93 M. Dai, L. Song, J. T. LaBelle and B. D. Vogt, *Chem. Mater.*, 2011, **23**, 2869.
94 L.-S. Zhang, W. Li, Z.-M. Cui and W.-G. Song, *J. Phys. Chem. C*, 2009, **113**, 20594.
95 C. Xiao, X. Chu, Y. Yang, X. Li, X. Zhang and J. Chen, *Biosens. Bioelectron.*, 2011, **26**, 2934.
96 S. A. Alharthi, T. E. Benavidez and C. D. Garcia, *Langmuir*, 2013, **29**, 3320.
97 R. Ye, Z. Peng, T. Wang, Y. Xu, J. Zhang, Y. Li, L. G. Nilewski, J. Lin and J. M. Tour, *ACS Nano*, 2015, **9**, 9244.
98 J. Lin, Z. Peng, Y. Liu, F. Ruiz-Zepeda, R. Ye, E. L. G. Samuel, M. J. Yacaman, B. I. Yakobson and J. M. Tour, *Nat. Commun.*, 2014, **5**, 5714.
99 A. C. Ferrari and J. Robertson, *Phys. Rev. B: Condens. Matter Mater. Phys.*, 2000, **61**, 14095.
100 A. C. Ferrari and J. Robertson, *Phys. Rev. B: Condens. Matter Mater. Phys.*, 2001, **64**, 075414.
101 A. C. Ferrari and J. Robertson, *Philos. Trans. R. Soc., A*, 2004, **362**, 2477.
102 S. F. Lux, E. Pollak, U. Boesenberg, T. Richardson and R. Kostecki, *Electrochem. Commun.*, 2014, **46**, 5.
103 M. Kakunuri and C. S. Sharma, *ECS Trans.*, 2015, **66**, 57.
104 K. Torbensen, J. Iruthayaraj, M. Ceccato, M. Kongsfelt, T. Breitenbach, S. U. Pedersen and K. Daasbjerg, *J. Mater. Chem.*, 2012, **22**, 18172.
105 M. G. Hahm, J.-H. Lee, A. H. C. Hart, S. M. Song, J. Nam, H. Y. Jung, D. P. Hashim, B. Li, T. N. Narayanan, C.-D. Park, Y. Zhao, R. Vajtai, Y. A. Kim, T. Hayashi, B.-C. Ku, M. Endo, E. Barrera, Y. J. Jung, E. L. Thomas and P. M. Ajayan, *ACS Nano*, 2013, **7**, 10971.
106 R. Martinez-Duarte, *Micromachines*, 2014, **5**, 766.
107 C. Liang, Z. Li and S. Dai, *Angew. Chem., Int. Ed.*, 2008, **47**, 3696.
108 R. C. Engstrom, *Anal. Chem.*, 1982, **54**, 2310.
109 S. A. Bhakta, E. Evans, T. E. Benavidez and C. D. Garcia, *Anal. Chim. Acta*, 2015, **872**, 7.
110 B. Hsia, M. S. Kim, M. Vincent, C. Carraro and R. Maboudian, *Carbon*, 2013, **57**, 395.
111 D. S. Hecht, L. Hu and G. Irvin, *Adv. Mater.*, 2011, **23**, 1482.
112 E. K. Walker, D. A. Vanden Bout and K. J. Stevenson, *Langmuir*, 2012, **28**, 1604.
113 G. M. Duran, T. E. Benavidez, J. G. Giuliani, A. Rios and C. D. Garcia, *Sens. Actuators, B*, 2016, **227**, 626.
114 R. Martinez-Duarte, F. Camacho-Alanis, P. Renaud and A. Ros, *Electrophoresis*, 2013, **34**, 1113.
115 R. L. McCreery and M. T. McDermott, *Anal. Chem.*, 2012, **84**, 2602.
116 M. Lu and R. G. Compton, *Analyst*, 2014, **139**, 4599.
117 M. Pumera, *Chem. Soc. Rev.*, 2010, **39**, 4146.
118 R. C. Alkire, P. N. Bartlett and J. Lipkowski, *Electrochemistry of Carbon Electrodes*, Wiley, 2015.
119 M. G. Jacob and J. S. Keith, in *Nanoelectrochemistry*, CRC Press, 2015, p. 293.
120 P. Chen and R. L. McCreery, *Anal. Chem.*, 1996, **68**, 3958.
121 D. A. C. Brownson, D. K. Kampouris and C. E. Banks, *Chem. Soc. Rev.*, 2012, **41**, 6944.
122 L. Amato, A. Heiskanen, R. Hansen, L. Gammelgaard, T. Rindzevicius, M. Tenje, J. Emnéus and S. S. Keller, *Carbon*, 2015, **94**, 792.
123 S. Sharma, R. Kamath and M. Madou, *J. Anal. Appl. Pyrolysis*, 2014, **108**, 12.
124 V. Penmatsa, H. Kawarada, Y. Song and C. Wang, *Mater. Sci. Res. India*, 2014, **11**, 1.
125 M. Santhiago, C. M. Maroneze, C. C. C. Silva, M. N. L. Camargo and L. T. Kubota, *ChemElectroChem*, 2015, **2**, 761.
126 D. Sánchez-Molas, J. Cases-Utrera, P. Godignon and F. Javier del Campo, *Sens. Actuators, B*, 2013, **186**, 293.
127 D. J. Fischer, M. K. Hulvey, A. R. Regel and S. M. Lunte, *Electrophoresis*, 2009, **30**, 3324.
128 T. Kobayashi, A. Akazawa, Y. Mori, Y. Furuno and S. Konishi, *Sens. Actuators, B*, 2013, **180**, 8.
129 C. D. García, C. P. De Pauli and P. I. Ortiz, *J. Electroanal. Chem.*, 2001, **510**, 115.
130 G. García, C. D. García, P. I. Ortiz and C. P. De Pauli, *J. Electroanal. Chem.*, 2002, **519**, 53.
131 P. A. Brooksby and A. J. Downard, *Langmuir*, 2004, **20**, 5038.
132 Y. R. Leroux, H. Fei, J.-M. Noël, C. Roux and P. Hapiot, *J. Am. Chem. Soc.*, 2010, **132**, 14039.
133 R. Nasraoui, J.-F. Bergamini, S. Ababou-Girard and F. Geneste, *J. Solid State Electrochem.*, 2011, **15**, 139.
134 A. J. Gross and A. J. Downard, *Anal. Chem.*, 2011, **83**, 2397.
135 P. Takmakov, M. K. Zachek, R. B. Keithley, P. L. Walsh, C. Donley, G. S. McCarty and R. M. Wightman, *Anal. Chem.*, 2010, **82**, 2020.
136 P. Ilanchezhiyan, J. J. Eo, A. S. Zakirov, S. D. Gopal Ram, G. N. Panin and T. W. Kang, *Mater. Lett.*, 2014, **124**, 18.
137 V. Řeháček, I. Hotový, M. Vojs, M. Kotlár, T. Kups and L. Spiess, *J. Electr. Eng.*, 2011, **62**, 49.
138 V. Rehacek, I. Hotovy, M. Vojs, T. Kups and L. Spiess, *Electrochim. Acta*, 2012, **63**, 192.
139 L. Moretto, A. Mardegan, M. Cettolin and P. Scopece, *Chemosensors*, 2015, **3**, 157.
140 M. Silvestrini, A. Mardegan, M. Cettolin, L. M. Moretto, P. Ugo and P. Scopece, in *Sensors*, ed. D. Compagnone, F. Baldini, C. Di Natale, G. Betta and P. Siciliano, Springer International Publishing, 2015, vol. 319, p. 135.
141 X. Xiao, G. A. Montaño, T. L. Edwards, C. M. Washburn, S. M. Brozik, D. R. Wheeler, D. B. Burckel and R. Polsky, *Biosens. Bioelectron.*, 2011, **26**, 3641.
142 Y. Huang, Y.-E. Miao, S. Ji, W. W. Tjiu and T. Liu, *ACS Appl. Mater. Interfaces*, 2014, **6**, 12449.

Published on 01 April 2016. Downloaded by Clemson University on 15/04/2016 14:03:16.

143 A. Mardegan, V. Pifferi, E. Pontoglio, L. Falciola, P. Scopece and L. M. Moretto, *Electrochem. Commun.*, 2014, **48**, 13.
144 X. Mao, X. Yang, G. C. Rutledge and A. T. Hatton, *ACS Appl. Mater. Interfaces*, 2014, **6**, 3394.
145 J.-H. Yang, V. Penmatsa, S. Tajima, H. Kawarada and C. Wang, *Mater. Lett.*, 2009, **63**, 2680.
146 O. Niwa and D. Kato, in *Nanobiosensors and Nanobioanalyses*, ed. C. M. d. Vestergaard, K. Kerman, I. M. Hsing and E. Tamiya, Springer, Japan, Tokyo, 2015, p. 121.
147 D. Liu, X. Zhang and T. You, *ACS Appl. Mater. Interfaces*, 2014, **6**, 6275.
148 V. Penmatsa, A. R. Ruslinda, M. Beidaghi, H. Kawarada and C. Wang, *Biosens. Bioelectron.*, 2013, **39**, 118.
149 V. Penmatsa, R. A. Rahim, H. Kawarada and C. Wang, *RSC Adv.*, 2015, **5**, 65042.
150 M. F. Mora, C. E. Giacomelli and C. D. Garcia, *Anal. Chem.*, 2009, **81**, 1016.
151 M. R. Nejadnik, F. L. Deepak and C. D. Garcia, *Electroanalysis*, 2011, **23**, 1462.
152 P. Batalla, A. Martín, M. Á. López, M. C. González and A. Escarpa, *Anal. Chem.*, 2015, **87**, 5074.
153 M. F. Mora, M. Reza Nejadnik, J. L. Baylon-Cardiel, C. E. Giacomelli and C. D. Garcia, *J. Colloid Interface Sci.*, 2010, **346**, 208.
154 M. Mora, J. Wehmeyer, R. Synowicki and C. Garcia, in *Biological Interactions on Materials Surfaces*, ed. D. A. Puleo and R. Bizios, Springer, US, 2009, p. 19.
155 T. E. Benavidez and C. D. Garcia, *Langmuir*, 2013, **29**, 14154.
156 T. E. Benavidez, D. Torrente, M. Marucho and C. D. Garcia, *J. Colloid Interface Sci.*, 2014, **435**, 164.
157 T. E. Benavidez, D. Torrente, M. Marucho and C. D. Garcia, *Langmuir*, 2015, **31**, 2455.
158 R. Martinez-Duarte, P. Renaud and M. J. Madou, *Electrophoresis*, 2011, **32**, 2385.
159 M. d. C. Jaramillo, E. Torrents, R. Martínez-Duarte, M. J. Madou and A. Juárez, *Electrophoresis*, 2010, **31**, 2921.
160 R. Martinez-Duarte, R. A. Gorkin III, K. Abi-Samra and M. J. Madou, *Lab Chip*, 2010, **10**, 1030.
161 M. d. C. Jaramillo, R. Martínez-Duarte, M. Hüttener, P. Renaud, E. Torrents and A. Juárez, *Biosens. Bioelectron.*, 2013, **43**, 297.
162 M. Elitas, R. Martinez-Duarte, N. Dhar, J. D. McKinney and P. Renaud, *Lab Chip*, 2014, **14**, 1850.
163 G. Mernier, R. Martinez-Duarte, R. Lehal, F. Radtke and P. Renaud, *Micromachines*, 2012, **3**, 574.
164 J. Cummins, J. Hull, K. Kitts and J. V. Goodpaster, *Anal. Methods*, 2011, **3**, 1682.
165 Z. Huang, P. E. Chua and H. K. Lee, *J. Chromatogr. A*, 2015, **1399**, 8.
166 J. W. Zewe, J. K. Steach and S. V. Olesik, *Anal. Chem.*, 2010, **82**, 5341.
167 J. E. Clark and S. V. Olesik, *J. Chromatogr. A*, 2010, **1217**, 4655.
168 M. F. Wahab, M. E. A. Ibrahim and C. A. Lucy, *Anal. Chem.*, 2013, **85**, 5684.
169 R. S. Deinhammer, E.-Y. Ting and M. D. Porter, *J. Electroanal. Chem.*, 1993, **362**, 295.
170 P. Nikitas, *J. Electroanal. Chem.*, 2000, **484**, 137.
171 B. J. Yakes, D. W. Keller and M. D. Porter, *J. Chromatogr. A*, 2010, **1217**, 4395.
172 D. A. Barrow, O. K. Castell, N. Sykes, P. Myers and H. Ritchie, *J. Chromatogr. A*, 2011, **1218**, 1983.
173 M. Pumera, *Chem. Rec.*, 2012, **12**, 201.
174 S. Zhao, H. Yin, L. Du, L. He, K. Zhao, L. Chang, G. Yin, H. Zhao, S. Liu and Z. Tang, *ACS Nano*, 2014, **8**, 12660.
175 T. E. Newsome and S. V. Olesik, *Anal. Chem.*, 2014, **86**, 10961.
176 H. Wang and S. V. Olesik, *J. Chromatogr. A*, 2015, **1379**, 56.
177 T. Lu and S. V. Olesik, *Anal. Chem.*, 2015, **87**, 3616.

 This journal is © The Royal Society of Chemistry 2016